CrossMark

ORIGINAL ARTICLE

Prediction of restrained shrinkage crack widths of slag mortar composites by Takagi and Sugeno ANFIS models

Turhan Bilir[1] · Osman Gencel[2] · Ilker Bekir Topcu[3]

Abstract Shrinkage is an important parameter affecting crack development of mortars and concrete. With the occurrence of shrinkage cracks, the concrete starts to be exposed to the corrosion which significantly decreases the durability of concrete or mortars. In this study, the results of free shrinkage tests determining the length changes and ring test determination of the restrained drying shrinkage cracks are used for predicting the crack widths of granulated blast furnace slag fine aggregate mortars using adaptive-network-based fuzzy inference system (ANFIS). Subsequently, replacement ratios, drying time and free shrinkage length changes are used as inputs and crack width as output in order to predict the shrinkage cracking of these mortar types. The experimental test and the prediction results from the ANFIS model are compared with each other. It is clear that ANFIS can be employed directly in the prediction or discussion of the drying shrinkage cracks.

Keywords ANFIS · Composite · Modeling · Mortar · Prediction · Restrained shrinkage cracking

✉ Osman Gencel
osmangencel@gmail.com

1 Department of Civil Engineering, Bülent Ecevit University, 67100 Zonguldak, Turkey

2 Department of Civil Engineering, Faculty of Engineering, Bartin University, 74100 Bartin, Turkey

3 Department of Civil Engineering, Eskişehir Osmangazi University, 26480 Eskisehir, Turkey

1 Introduction

1.1 Drying shrinkage and cracking

Cracks occur on concrete surfaces due to the restrained shrinkage that leads to increment in permeability and porosity in cement-based products like mortar and concrete because of tensile stresses. Also, mechanical and durability properties of them decrease with the ingress of external materials through these cracks. The shrinkage is affected by the joint properties of cement paste, aggregate and admixtures. Cement paste properties affecting the shrinkage are porosity, age and degree of hydration. Besides, w/c ratio, curing conditions (temperature, humidity, etc.), cement, aggregate and water contents are the concrete properties affecting shrinkage in addition to the admixture type. Furthermore, among the aggregate properties are the stiffness, volume to surface ratio and size. When pozzolanic mineral admixture properties are considered, the pozzolanic reactivity, fineness and water absorption ratio are the common ones affecting the shrinkage and shrinkage cracking. On the other hand, the chemical admixtures affect shrinkage by water or porosity reduction and strength increment capabilities. Additionally, environmental conditions such as relative humidity, drying rate and time have also considerable significant effects on shrinkage cracking [1, 2].

Shrinkage generally increases with higher strength and lower porosity with elapsed time due to the use of pozzolanic mineral admixtures in concrete. They may also cause reduction in shrinkage related to the other properties of mineral admixture. For instance, the usage of fly ash provided from Afşin-Elbistan Thermal Power Plant, Turkey, decreases shrinkage of concrete [3]. However, it can be said that this occurs for only replacements below 30 %

Springer

ratio during early ages. Fly ash (FA) increases drying shrinkage cracking at later ages due to the higher water absorption [4–6].

The mineral admixtures such as fly ash decrease early-age shrinkage and cracking by reducing the cement paste content [7]. It is reported that FA as fine aggregate decreases shrinkage cracking regarding the properties like water absorption and w/c ratios [8]. It is also clear that the cement paste content and w/c ratio are the most important parameters affecting shrinkage because of their effects on hydration, water content, compressive strength and elastic properties [9, 10].

Besides, rubber aggregate effect on shrinkage cracking can be given as an example in order to underline the significant effect of elastic properties on shrinkage. Rubber aggregate delays and decreases shrinkage cracking due to the decrease in the concrete elasticity moduli [11]. In addition to these properties, it is also seen that drying media and rate are other important parameters [12]. When the shrinkage of concrete is restrained during drying process, internal tensile stresses occur. If these tensile stresses exceed the tensile strength of mortar or concrete, drying shrinkage crack formation can be seen [4]. The best solution to reduce drying shrinkage cracking is believed to be the higher tensile strength and lower modulus of elasticity [4]. Some techniques such as the use of optical or scanning electron microscopes (SEM) are developed to measure and investigate these crack formations [13]. Moreover, the cheapest method to form and measure these cracks can be said as "the ring test" [14].

The industrial by-products or the solid wastes such as FA, bottom ash, slag, silica fume and waste glass can also be used as mineral admixture or as fine aggregate in concrete in order to improve some properties of concrete or mortars, while other properties can be affected negatively [15–21]. For instance, GBFS usage as fine aggregate can make it possible to produce durable concrete due to its mechanical, physical and chemical properties even if this reduces the compressive or flexural strengths due to its physical properties [15–17]. The reason for the decrease in mechanical properties due to the GBFS usage is determined as the porosity and permeability increase by evaluating the SEM images of such concrete types incorporating GBFS fine aggregates at different amounts [17, 21]. However, conducted tests have also presented that chemical and other physical properties can improve durability properties [15, 17, 21]. Furthermore, GBFS may also decrease free and restrained shrinkage due to the porous microstructure occurrences.

Some effects such as curing aggregate type, incorporation of shrinkage-reducing admixture on cracking of alkali-activated slag concretes are also investigated [22]. Blast furnace slag aggregate has caused to the lower drying shrinkage, higher tensile strength and lower modulus of elasticity in alkali-activated slag concretes and, thus, reduced drying shrinkage cracking [22]. Among all these studies, it is reported that the shrinkage cracking depends on shrinkage potential and rate, tensile creep, tensile strength and the degree of restraint [23, 24]. Besides, the shrinkage-reducing admixtures significantly decrease drying shrinkage cracking [23, 24]. Additionally, it is observed that the increase in the size of fine aggregate decreases the long-term drying shrinkage of mortars [25]. Furthermore, the specimen size and shape have also significant effects on drying shrinkage of concrete [26]. In other words, the test specimen type is very important for determining the drying shrinkage or the drying shrinkage cracking. The use of fibers also decreases the drying shrinkage crack widths of mortars produced with recycled aggregates even if the recycled aggregates increase the drying shrinkage of mortars [27]. The increase in fiber content increases the strain capacity and decreases the drying shrinkage cracking potential [28]. However, the type of the fiber can decrease the drying shrinkage cracking [29]. On the other hand, the fiber content may not resist higher shrinkage-induced tensile stresses in lightweight aggregate concrete [30]. There are also some studies conducted about the shrinkage cracking of high-strength concrete [31]. High-strength concrete is more sensitive to the drying shrinkage cracking [32]. In addition to these statements, the simple solution to reduce drying shrinkage can be said as long curing periods [32]. Finally, high-performance or high-strength concrete types are evaluated in terms of drying shrinkage and it is reported that the drying shrinkage of high-performance lightweight concrete can change based on the curing period [33, 34]. However, the studies about drying shrinkage and restrained drying shrinkage cracking of lightweight aggregate concretes or mortars are rather limited than the normal ones.

1.2 Shrinkage modeling

In one of the previous studies about predicting the shrinkage behavior of concrete, shrinkage strains are estimated by using some statistical methods such as CEB-FIP 1990, EHE, ACI 209R, B3 and GL200 (empirical shrinkage prediction methods) for both self-consolidating concrete and conventional concrete [35]. In this way, ACI 209R-92 model includes the effects of the moist curing, steam curing, ambient relative humidity, member size, concrete composition, slump, fine aggregate, cement and air contents on ultimate drying shrinkage [35]. CEB-FIP 1990 predicts the drying shrinkage strain using compressive strength, cement type, member cross-sectional area, relative humidity and concrete age [35]. EHE model is based on the CEB-FIP 1990 model, and it does not include

cement type [35]. B3 and GL2000 models are also similar to CEB-FIP 1990 model, and they predict the drying shrinkage strain using similar parameters with some additional or different coefficients and parameters [35]. In the conclusions of this study, it is reported that all types of empirical estimation methods are effective for both self-consolidating concrete and conventional concrete [35]. On the other hand, ACI 209R model is the best model for estimating drying shrinkage strain in terms of statistical analysis [35]. In another study, a nonlinear diffusion equation is used to obtain a statistical model applicable for all kinds of geometry and concrete under variable ambient conditions by the prediction of the concrete beam structure shrinkage strains in terms of moisture content and the weight loss [36]. Collins and Sanjayan [37] have developed a numerical model for alkali-activated slag concrete beams subjected to restrained shrinkage, which is a stress-based model including shrinkage, elastic modulus, creep, tensile strength and time.

The long-term ultimate shrinkage strain can also be developed by using ACI shrinkage prediction models and parameters that can be obtained from short-term shrinkage strain tests [38]. Besides, shrinkage stresses of mortar specimens are determined using rubber models to predict the shrinkage cracking in concrete building walls indicating the restraint type [39]. AS 1481, AS 3600, Bazant, CEB90 and NAASRA shrinkage prediction methods are also comparable with each other and ACI 209 by using data obtained from 46 Australian concretes with over 1500 points using the method of residual plotting [40], which are based on empirical and statistical methods. Besides, some other models are available to predict the shrinkage strains of different types of concretes. These concrete types have different types of geometries, compositions or ambient conditions, etc. In other words, these previous models are using different parameters as input and output. Additionally, the statistical or other modern methods are used for constructing such shrinkage strain predicting models. For instance, a drying shrinkage strain prediction model is developed with respect to constant relative humidity and temperature conditions for various periods of curing time [41]. A creep and drying shrinkage prediction model considering compressive strength and modulus of elasticity is also developed [42]. Besides, coefficients of ACI 209 R92 model indicating creep, shrinkage and modulus of elasticity are also modified for high-performance concretes to predict the drying shrinkage strain [43]. However, it is reported that two common models as ACI and CEB-FIP are available for a wide range of different concrete mixtures but not for cement pastes, mortars or any fiber-reinforced materials [44]. These models can also be modified for cementitious composites using modulus of elasticity of concrete at the initial load, age of concrete after mixing, age concrete at

loading, ultimate specific creep in predicting creep strains or using coefficients related to shrinkage and the age of concrete at the beginning of shrinkage and the age of concrete in predicting the drying shrinkage strain [44].

All of these models attempt to predict or estimate the creep or drying shrinkage strains using different properties such as mechanical, elastic, curing properties and exposure periods and times. The most common properties used for developing drying shrinkage strain prediction models can be said as moisture content, relative humidity, modulus of elasticity, the age of the specimen, the shape and the size of the specimen, compressive strength, restraint conditions, curing conditions, exposure time, etc. [35–44]. There are limited numbers of studies investigating the development of models predicting or estimating the drying shrinkage cracking. Most of them focus on the cracking of concrete members by predicting the crack widths of these members [45, 46]. Only one of the available studies in the literature was about the drying shrinkage cracks and the ring specimens [47]. The theoretical model in this study depends on the nonlinear fracture mechanics related to fracture energy rather than the tensile strength. This model includes the fracture resistance curve, strain energy, maximum allowable tensile strain and the prediction of the age for transverse cracking of the ring [47].

1.3 The aim and scope of this study

In this study, ANFIS is used in order to predict the drying shrinkage crack widths of mortars containing nonground GBFS as fine aggregate. ANFIS is a common modern scientific prediction method. It has the capability to reflect the effects of linguistic parameters like fuzzy logic (FL) and the learning capacity of neural networks. ANFIS has many application areas including the prediction of some concrete properties [48–52]. ANFIS is one of the modern scientific methods which became common because of its combined properties of artificial neural networks (ANN) and fuzzy logic. It has the ability of employing linguistic parameters like fuzzy logic, and it has the property of learning like artificial neural networks. Statistical methods require enough amount of numerical input for model to represent all parameters. However, ANN and fuzzy logic do not require too many data or input. Besides, ANN can learn and weight the parameters in order to simulate the effects of the parameters on output. Thus, every new data (experimental or observation data) make the model to represent all actual effects and their weights on output. Therefore, each of the data makes model prediction more precise. On the other hand, fuzzy logic can represent the linguistic parameters which cannot be expressed by numbers as data. Therefore, some linguistic data from experience can also be reflected to the model. This cannot be seen

in statistical methods. Finally, ANFIS has these two abilities in order to obtain a more precise model. Besides, this study is a significant example for ANFIS model usage in predicting the restrained drying shrinkage crack widths of GBFS mortars related to the ring test. The replacement ratios of GBFS as fine aggregate in mortars (RR), the drying time of ring specimens (DT), the free shrinkage length changes of GBFS mortars (FS) are used as inputs, and the crack widths of GBFS mortars (CW) exposed to ring test are used as output. Besides, models indicated in the previous literature are empirical and statistical methods. There are not any neuro-fuzzy inference models predicting the drying shrinkage or the shrinkage cracking given in the literature even if there are some studies developing prediction models for other properties of concrete by using neural networks and fuzzy logic models. Thus, this study provides an innovative application of ANFIS method on developing a prediction model for drying shrinkage crack widths of GBFS fine aggregate mortars using replacement ratio, drying period and length changes.

2 ANFIS: adaptive-network-based fuzzy inference system

Before constructing the model, the properties of ANFIS should generally be discussed. First of all, ANFIS is capable for approximating any real continuous function on a compact set to any degree of accuracy [48, 49]. In other words, there are almost no restraints on the node functions of an adaptive network except piecewise differentiability. The only limitation of network configuration is of feedforward type. Thus, the adaptive network applications are commonly used in various areas. The proposed architecture is referred to as ANFIS, standing for adaptive-network-based fuzzy inference system [50]. When the data are the measurable system variables with an internal system parameter, a functional mapping may be constructed by ANFIS that approximates the process of estimation of the internal system parameter. ANFIS is a soft computing technique which incorporates the concept of fuzzy logic into the neural networks. ANFIS can simulate and analyze the mapping relation between the input and output data through a hybrid learning to determine the optimal distribution of membership function [49]. It is mainly based on the fuzzy "if–then" rules from the Takagi and Sugeno fuzzy model [48]. It involves a premise part and a consequent part. The typical architecture of ANFIS can be seen in Fig. 1. It has five layers in this inference system, and each layer involves several nodes, called as the node function [49].
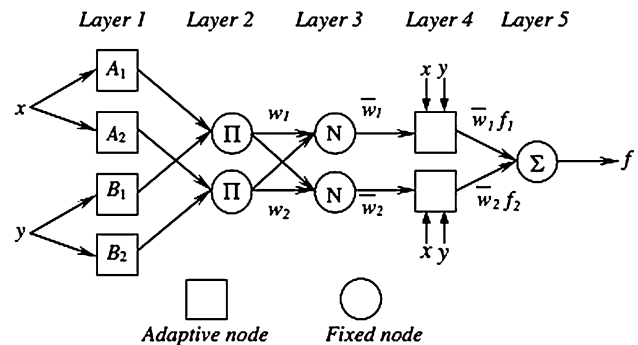

Fig. 1 The architecture of ANFIS [48, 49]

2.1 ANFIS architecture

The common use of ANFIS type can be said as Takagi and Sugeno's type [51, 52]. For this type of fuzzy inference system (FIS), as mentioned above, there are five layers and nodes in each layer. These layers are discussed below. First of all, if there are two inputs x and y and one output z. Two fuzzy if–then rules can be given as follows [50].

> Rule 1: If x is A_1 and y is B_1, then $f_1 = p_1x + q_1y + r_1$.
> Rule 2: If x is A_2 and y is B_2, then $f_2 = p_2x + q_2y + r_2$.

In rules 1 and 2, x and y are the inputs, A_i and B_i are the fuzzy sets, f_i are the outputs within the fuzzy region specified by the fuzzy rule. p_i, q_i and r_i are the design parameters that are determined during the training process. The input variables x and y affecting the output variable of the model f have different values, f also has different values, and thus, the design parameters of p, q and r are also have different values. For instance, x varies from A_1 to A_2 and y varies from B_1 to B_2 and the output f also varies from f_1 to f_2; then, the p_1, q_1 and r_1 become p_2, q_2 and r_2. In this case, the model adapts itself and determines the design parameters for each input variable. In other words, the model weights the effects of the factors (variables) and calculates the design parameters p_i, q_i and r_i related to the effect level of inputs x and y. This means that the model learns the effects of all input variables and determines the design parameters related to the contributions of inputs on the output. Therefore, the effect of an input on output can be weighted and the actual effect can be reflected to the output. Finally, it can be said that after training process, the more effective input variable or the effect percent of each input variable can be seen from the values of design parameters p_i, q_i and r_i.

The node functions in the same layer are of the same function family as described below:

Layer 1 Every node i in this layer is a square node with a node function.

$$Q_i^1 = \mu_{A_i}(x) \tag{1}$$

where x is the input to node i and A is the linguistic label ("small", "large", etc.) associated with this node function. x is usually be chosen to be bell-shaped with maximum membership degree (MD) equal to 1 and minimum equal to 0, such as

$$\mu_{A_i}(x) = \frac{1}{1 + \left[\left(\frac{x-c_i}{a_i}\right)\right]^{b_i}} \quad \text{or} \quad \mu_{A_i} = \exp\left\{-\left(\frac{x-c_i}{a_i}\right)^2\right\} \tag{2}$$

where $\{a_i, b, c_i\}$ is the parameter set. As the parameter values change, the bell-shaped functions vary accordingly, thus exhibiting various forms of membership functions (MFs) on linguistic label A_i. In fact, any continuous and piecewise differentiable functions, such as commonly used trapezoidal- or triangular-shaped MFs, are also qualified candidates for node functions in this layer. Parameters in this layer are referred to as premise parameters [51].

Layer 2 Every node in this layer is a circle node labeled T_z which multiplies the incoming signals and sends the product out. For instance, each node output represents the firing strength of a rule.

$$w_i = \mu_{A_i}(x) \times \mu_{B_i}(y), \quad i = 1, 2. \tag{3}$$

Layer 3 Every node in this layer is a circle node labeled N. The ith node calculates the ratio of the ith rule's firing strength to the sum of all rules firing strengths:

$$\overline{w_i} = \frac{w_i}{w_1 + w_2}, \quad i = 1, 2. \tag{4}$$

For convenience, outputs of this layer will be called normalized firing strengths.

Layer 4 Every node i in this layer is a square node with a node function:

$$Q_i^4 = \overline{w_i} f_i = \overline{w_i}(p_i x + q_i y + r_i) \tag{5}$$

where W_i is the output of layer 3 and $\{p_i, q_i, r_i\}$ is the parameter set.

Layer 5 The single node in this layer is a circle node labeled C that computes the overall output as the summation of all incoming signals, i.e.,

$$Q_1^5 = \text{overall\_output} = \sum \overline{w_i} fi = \frac{\sum w_i f_i}{\sum w_i} \tag{6}$$

Thus, an adaptive network, which is functionally equivalent to a type-3 FIS, has been constructed. For type-1 fuzzy inference systems, the extension is quite straightforward. For type-2 fuzzy inference systems, if the centroid defuzzification operator with a discrete version which calculates the approximate centroid of area is replaced,

then type-3 ANFIS can still be constructed accordingly. However, it will be more complicated than its type-3 and type-1 versions and thus not worth the efforts to do so [50].

The learning mechanisms should not be applied to the determination of MFs since they convey linguistic and subjective description of ill-defined concepts. This is a case-by-case situation, and the decision should be left to the users. In principle, if the size of available input–output data set is large enough, then the fine-tuning of the MFs is applicable since the human-determined MFs are subject to the differences from person to person and from time to time; therefore, they are rarely optimal in terms of reproducing desired outputs. However, if the data set is too small, then it probably does not contain enough information of the system under consideration. In this situation, the human-based MFs represent important knowledge obtained through human experts' experiences and it might not be reflected in the data set; therefore, the MFs should be kept fixed throughout the learning process [50].

Interestingly enough, if the MFs are fixed and only the consequent part is adjusted, the ANFIS can be viewed as a functional-link network where the "enhanced representation" of the input variables is achieved by the MFs [50].

2.2 Fuzzy inference systems (FIS) with simplified fuzzy if–then rules

For type-1 reasoning, the MFs on the consequence part are restricted to monotonic functions which are not compatible with linguistic terms such as "medium" having bell-shaped MF. For type-2 reasoning, the defuzzification process is time-consuming and systematic fine-tuning of the parameters is not easy. For type-3 reasoning, it is just hard to assign any appropriate linguistic terms to the consequence part which is a nonfuzzy function of the input variables. To cope with these disadvantages, simplified fuzzy if–then rules of the following form are introduced:

If x is big and y is small, then z is d.

z is described by a crisp value (or equivalently, a singular MF). This class of simplified fuzzy if–then rules can employ all three types of reasoning mechanisms. More specifically, the consequent part of this simplified fuzzy if–then rule is represented by a step function (centered at $z = d$) in type 1, a singular MF (at $z = d$) in type 2 and a constant output function in type 3, respectively. Thus, the three reasoning mechanisms are unified under these simplified fuzzy if–then rules [50].

2.3 The basic of Takagi–Sugeno fuzzy logic

Takagi–Sugeno fuzzy logic or Sugeno fuzzy logic has first been introduced in 1985 [43–45]. It is the modification of

Mamdani model. Fuzzifying the inputs and applying the fuzzy operation are exactly the same to Mamdani model. The different place between them is the output MF. Sugeno-type output MFs are either linear functions or constants.

When the output functions are constant, it can be called as zero-order Sugeno fuzzy model. For example, a zero-order Sugeno fuzzy logic can be defined as:

If x is A and y is B, then $z = k$.

where A and B are fuzzy set defined for the MFs for x and y. k is a constant crisp value defined in the consequent. Therefore, the output of each rule is like a spike. The operator of implication and aggregation methods is simply multiplication and addition. A first-order Sugeno fuzzy logic model has the rules like that:

If x is A and y is B, then $z = px + qy + r$.

where A and B are fuzzy sets in the antecedent, while p, q and r are all the constants. The location is defined by the input data. This makes the system efficiently and compactly respond the change of input. Higher-order models are possible, but they become more complex and just have little more advantage [50–52].

3 ANFIS method application

In this study, the restrained shrinkage crack widths of nonground GBFS fine aggregate mortars are attempted to be predicted by using ANFIS method. The required data are obtained from an experimental study conducted by Eskişehir Osmangazi University Materials of Construction Division. The related experimental procedure is only given, and the model construction is explained according to the study objective. In this manner, the experimental free shrinkage test and ring test results are given as the comparison of the predicted and the experimental results.

In the related experimental study, GBFS is used in nonground form as fine aggregate and CEM II/B-M 32.5-type cement as hydraulic binder. CEN reference natural sand (CEN standard sand) corresponding TS EN 196-1 [53] and super-plasticizer as chemical admixture are the other mixing materials in mortar production. Eskişehir tap water is used as mixing water, and mortar specimens are produced for shrinkage cracking observations and experimental measurements. A reference mixture is designed using only CEN reference sand. The other specimens are produced by replacing sand with GBFS by weight at the ratios of 10, 20, 30, 40, 50, 60, 70, 80, 90 and 100 %. Length changes due to free shrinkage and width changes of restrained shrinkage cracks are determined by conducting required tests on these specimens.

Produced mortar specimens for free shrinkage test are kept under 20 °C temperatures and 90 % relative humidity during 24 h. After then, the cast was demolded and the length changes are measured, while the specimens are kept under 23 ± 2 °C temperature and 50 ± 4 % relative humidity during 60 days according to ASTM C 157 [54]. Ring-type specimens are prepared for restrained shrinkage cracking test, and kept under same conditions like free shrinkage specimens as 23 ± 2 °C temperature and 50 ± 5 % relative humidity during 60 days. The reason of exposing free or shrinkage specimens to these drying conditions is to obtain the maximum shrinkage effect related to the previous knowledge, and that is why ASTM C 157 [54] suggests these conditions. These drying conditions are provided by using the drying conditions in the room checked by using an electronic device capable for measuring temperature and humidity four times before the evening with the time interval of 3 h during the free shrinkage and ring tests. The upper surface of the specimen is sealed with silicon material to avoid exposure of the drying effect of the conditions to this upper surface. Thus, the circular surface could only be exposed to drying or curing conditions. Henceforth, the crack formation and development are observed during 60 days, and crack widths are measured everyday by using optical crack microscope on the ring test specimens. The dimensions of the ring mold for determining restrained shrinkage cracking are presented in Fig. 2. Ring test setup is presented in Fig. 3.

In the construction of ANFIS model, RR of GBFS, DT of ring specimens and the experimental FS results of specimens are considered as input and the shrinkage CW is used as output to train and test the model, and hence, totally 456 data are obtained. The experimental results leading no cracks are not used in the models. The RR, DT and FS inputs are composed of only the data having crack formation in order to improve the precision of the model. Among all the data, only 238 of them are used for training the model and 120 of them are reserved for testing. The testing data are approximately 33 %. The reason is that ANFIS model suggests 33 % of the data to be used as testing data [50]. The training data are given in Table 1, and the testing data are presented in Table 2. Three inputs and one output are used to construct the ANFIS model. Besides, Takagi–Sugeno-type ANFIS model and grid partition method are used to generate FIS. In the next process, hybrid method and ten epochs are applied. However, two epochs were enough to train the model. Five constant Gaussian MFs are chosen for inputs during the training process. The reason for these choices is to obtain the best solution by using them. Some of the methods such as subclustering and grid partition and some types of MFs such as Gaussian, sigmoid, triangular and trapezoidal are tried, and

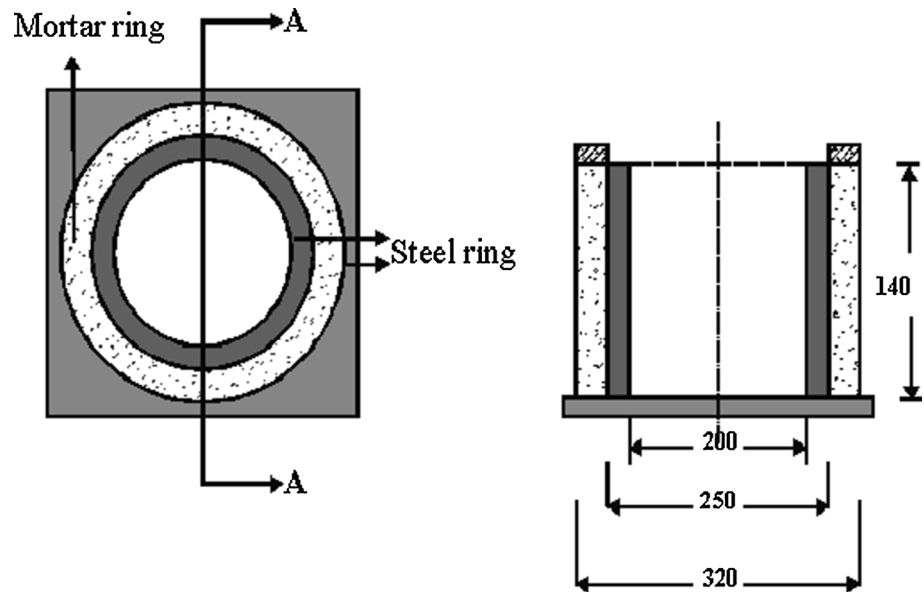**Fig. 2** Dimensions (mm) of the ring test setup

Fig. 3 The ring test setup for restrained shrinkage cracking

the best choice is the model including the Gaussian MF and the grid partition method with the parameters chosen as mentioned above. In other words, different models with different parameters are tried and this model was chosen because of the best performance obtained compared with the other models. The performance comparison of the models constructed to obtain the best performance is represented in Table 3. For some models in which sub-clustering method used, better root-mean-square error (RMSE) and the absolute fraction of variance (R^2) are obtained. However, the MFs of other models are not available for use because of the irregular distribution of FS MF. The MFs of the chosen model are preferable in the point of the view of the fuzzy philosophy. The chosen ANFIS model with five

constant Gaussian MFs and grid partition method is coded as grid1. The schematic demonstration of the ANFIS model coded as grid1 is shown in Fig. 4. Totally, 125 rules are obtained and the structure of the model is presented in Fig. 5. The RR as input1 and the DT as input2 have regular MFs as Gaussian behavior. On the other hand, the FS as input 3 has irregular MF distribution. This may be due to the nature of mortars incorporating GBFS fine aggregate having more granular physical structure and coarser gradation than the reference sand.

4 Results and discussion

Figure 6 presents the experimental and prediction results after training the model, and Fig. 7 shows the comparison between these results after testing. It is seen that the prediction and experimental results for the data are rather close to each other. On the other hand, the differences between these results can be relatively higher for some of the data in both training and testing phases. Besides, the prediction result can have negative values for one or two data. However, these data are limited for both processes, especially in the training process due to the mechanism of ANFIS modeling. The numbers of predicted and experimental results have relatively higher differences in testing than the training phase. Additionally, the maximum difference between the prediction and experimental results is 0.0565 mm and the maximum difference for testing is about 0.0849 mm. These differences for a few data can be unacceptable and may occur because of the irregular experimental free shrinkage length distribution, which is obtained due to the porous structure with increase in GBFS

Table 1 Training data

RR (%)	DT (day)	FSH (mstr.)	CW (mm)	RR (%)	DT (day)	FSH (mstr.)	CW (mm)	RR (%)	DT (day)	FSH (mstr.)	CW (mm)
0	19	0.002095	0.110	10	21	0.002705	0.173	20	21	0.002752	0.271
0	21	0.002182	0.630	10	22	0.002733	0.520	20	22	0.002795	0.465
0	22	0.002295	0.990	10	24	0.002789	0.941	20	24	0.002950	0.766
0	24	0.002361	1.197	10	25	0.002835	0.987	20	25	0.003150	0.862
0	25	0.002408	1.210	10	27	0.002860	1.004	20	27	0.003172	0.908
0	27	0.002446	1.221	10	28	0.002884	1.008	20	28	0.003171	0.913
0	28	0.002533	1.227	10	30	0.002944	1.026	20	30	0.003185	0.921
0	30	0.002551	1.248	10	31	0.002954	1.030	20	31	0.003254	0.934
0	31	0.002600	1.252	10	33	0.002961	1.038	20	33	0.003459	0.940
0	33	0.002628	1.262	10	34	0.002968	1.041	20	34	0.003880	0.945
0	34	0.002691	1.263	10	36	0.003021	1.047	20	36	0.003754	0.949
0	36	0.002660	1.269	10	37	0.003053	1.049	20	37	0.003654	0.953
0	37	0.002649	1.270	10	39	0.003056	1.056	20	39	0.003701	0.957
0	39	0.002698	1.282	10	40	0.003095	1.063	20	40	0.003715	0.961
0	40	0.002733	1.287	10	42	0.003130	1.063	20	42	0.003796	0.966
0	42	0.002754	1.289	10	43	0.003126	1.065	20	43	0.003769	0.968
0	43	0.002754	1.290	10	45	0.003154	1.066	20	45	0.003775	0.970
0	45	0.002779	1.292	10	46	0.003179	1.068	20	46	0.00378	0.970
0	46	0.002811	1.292	10	48	0.003196	1.069	20	48	0.003775	0.972
0	48	0.002842	1.294	10	49	0.003239	1.069	20	49	0.003752	0.973
0	49	0.002842	1.294	10	51	0.003249	1.071	20	51	0.003793	0.974
0	51	0.002881	1.298	10	52	0.003295	1.073	20	52	0.003765	0.974
0	52	0.002860	1.299	10	54	0.003435	1.074	20	54	0.003789	0.977
0	54	0.002898	1.300	10	55	0.003418	1.074	20	55	0.003798	0.977
0	55	0.002881	1.300	10	57	0.003544	1.074	20	57	0.003752	0.978
0	57	0.002905	1.300	10	58	0.003579	1.074	20	58	0.003742	0.978
0	58	0.002863	1.300	10	60	0.003502	1.074	20	60	0.003798	0.978
0	60	0.002926	1.300	10	21	0.002705	0.173				
RR (%)	DT (day)	FSH (mstr.)	CW (mm)	RR (%)	DT (day)	FSH (mstr.)	CW (mm)	RR (%)	DT (day)	FSH (mstr.)	CW (mm)
30	24	0.001589	0.342	40	25	0.001809	0.044	50	30	0.000911	0.083
30	25	0.001601	0.401	40	27	0.001869	0.462	50	31	0.000919	0.250
30	27	0.001615	0.635	40	28	0.001894	0.485	50	33	0.000921	0.471
30	28	0.001618	0.660	40	30	0.001983	0.500	50	34	0.000935	0.474
30	30	0.001652	0.671	40	31	0.002053	0.502	50	36	0.000941	0.482
30	31	0.001682	0.674	40	33	0.002235	0.501	50	37	0.000943	0.484
30	33	0.001792	0.686	40	34	0.002321	0.501	50	39	0.000964	0.493
30	34	0.001865	0.689	40	36	0.002445	0.501	50	40	0.000936	0.495
30	36	0.001924	0.695	40	37	0.002432	0.501	50	42	0.000985	0.499
30	37	0.001952	0.697	40	39	0.002436	0.501	50	43	0.000999	0.500
30	39	0.002026	0.700	40	40	0.002456	0.501	50	45	0.001000	0.502
30	40	0.002030	0.702	40	42	0.002465	0.501	50	46	0.001002	0.503
30	42	0.002038	0.706	40	43	0.002402	0.501	50	48	0.001022	0.505
30	43	0.002042	0.711	40	45	0.002439	0.501	50	49	0.001020	0.508
30	45	0.002050	0.711	40	46	0.002456	0.501	50	51	0.001017	0.511
30	46	0.002062	0.712	40	48	0.002482	0.501	50	52	0.001015	0.511
30	48	0.002083	0.713	40	49	0.002467	0.501	50	54	0.001025	0.512
30	49	0.002098	0.714	40	51	0.002485	0.501	50	55	0.001025	0.512
30	51	0.002234	0.715	40	52	0.002498	0.501	50	57	0.001025	0.513

Table 1 continued

RR (%)	DT (day)	FSH (mstr.)	CW (mm)	RR (%)	DT (day)	FSH (mstr.)	CW (mm)	RR (%)	DT (day)	FSH (mstr.)	CW (mm)
30	52	0.002258	0.715	40	54	0.002501	0.501	50	58	0.001025	0.513
30	54	0.002288	0.716	40	55	0.002488	0.501	50	60	0.001029	0.513
30	55	0.002292	0.717	40	57	0.002496	0.501	50	30	0.000911	0.083
30	57	0.002302	0.718	40	58	0.002513	0.501				
30	58	0.002315	0.719	40	60	0.002475	0.501				
30	60	0.002302	0.719								

RR (%)	DT (day)	FSH (mstr.)	CW (mm)	RR (%)	DT (day)	FSH (mstr.)	CW (mm)	RR (%)	DT (day)	FSH (mstr.)	CW (mm)
60	33	0.001953	0.035	70	34	0.002482	0.012	80	34	0.002458	0.008
60	34	0.001982	0.185	70	36	0.002492	0.067	80	36	0.002467	0.045
60	36	0.002119	0.335	70	37	0.002496	0.166	80	37	0.002471	0.111
60	37	0.002139	0.352	70	39	0.002504	0.201	80	39	0.002479	0.134
60	39	0.002253	0.358	70	40	0.002503	0.203	80	40	0.002478	0.136
60	40	0.002260	0.359	70	42	0.002504	0.205	80	42	0.002479	0.137
60	42	0.002264	0.366	70	43	0.002504	0.206	80	43	0.002479	0.137
60	43	0.002264	0.367	70	45	0.002505	0.210	80	45	0.002480	0.140
60	45	0.002285	0.370	70	46	0.002506	0.210	80	46	0.002481	0.140
60	46	0.002352	0.371	70	48	0.002506	0.212	80	48	0.002481	0.141
60	48	0.002432	0.372	70	49	0.002506	0.212	80	49	0.002481	0.141
60	49	0.002446	0.373	70	51	0.002508	0.213	80	51	0.002483	0.142
60	51	0.002437	0.375	70	52	0.002509	0.213	80	52	0.002484	0.142
60	52	0.002468	0.377	70	54	0.002512	0.215	80	54	0.002487	0.144
60	54	0.002489	0.379	70	55	0.002515	0.216	80	55	0.002490	0.144
60	55	0.002490	0.379	70	57	0.002519	0.217	80	57	0.002493	0.144
60	57	0.002503	0.380	70	58	0.002519	0.217	80	58	0.002494	0.144
60	58	0.002512	0.380	70	60	0.002520	0.217	80	60	0.002496	0.145
60	60	0.002526	0.380								

RR (%)	DT (day)	FSH (mstr.)	CW (mm)	RR (%)	DT (day)	FSH (mstr.)	CW (mm)
90	39	0.002726	0.009	100	40	0.002808	0.003
90	40	0.002726	0.030	100	42	0.002808	0.019
90	42	0.002726	0.084	100	43	0.002808	0.029
90	43	0.002727	0.089	100	45	0.002810	0.056
90	45	0.002728	0.090	100	46	0.002811	0.057
90	46	0.002729	0.090	100	48	0.002811	0.057
90	48	0.002729	0.092	100	49	0.002811	0.058
90	49	0.002729	0.092	100	51	0.002814	0.059
90	51	0.002732	0.093	100	52	0.002815	0.059
90	52	0.002733	0.093	100	54	0.002818	0.059
90	54	0.002736	0.094	100	55	0.002821	0.059
90	55	0.002739	0.094	100	57	0.002825	0.060
90	57	0.002743	0.094	100	58	0.002825	0.060
90	58	0.002743	0.095	100	60	0.002828	0.060
90	60	0.002746	0.095				

Table 2 Testing data

RR (%)	DT (day)	FSH (mstr.)	CW (mm)	RR (%)	DT (day)	FSH (mstr.)	CW (mm)	RR (%)	DT (day)	FSH (mstr.)	CW (mm)
0	20	0.002140	0.210	10	20	0.002653	0.091	20	23	0.002765	0.545
0	23	0.002340	1.140	10	23	0.002796	0.817	20	26	0.003160	0.898
0	26	0.002411	1.217	10	26	0.002909	0.998	20	29	0.003180	0.917
0	29	0.002554	1.243	10	29	0.002912	1.012	20	32	0.003421	0.937
0	32	0.002568	1.258	10	32	0.002961	1.033	20	35	0.003877	0.948
0	35	0.002663	1.267	10	35	0.003004	1.043	20	38	0.003685	0.955
0	38	0.002719	1.275	10	38	0.003049	1.051	20	41	0.003734	0.968
0	41	0.002730	1.288	10	41	0.003112	1.062	20	44	0.003770	0.969
0	44	0.002796	1.291	10	44	0.003126	1.066	20	47	0.003780	0.972
0	47	0.002832	1.293	10	47	0.003189	1.068	20	50	0.003812	0.973
0	50	0.002860	1.295	10	50	0.003246	1.070	20	53	0.003772	0.976
0	53	0.002860	1.299	10	53	0.003330	1.074	20	56	0.003774	0.978
0	56	0.002888	1.300	10	56	0.003530	1.074	20	59	0.003798	0.978
0	59	0.002916	1.300	10	59	0.003558	1.074				

RR (%)	DT (day)	FSH (mstr.)	CW (mm)	RR (%)	DT (day)	FSH (mstr.)	CW (mm)	RR (%)	DT (day)	FSH (mstr.)	CW (mm)
30	23	0.001532	0.199	40	26	0.001865	0.401	50	29	0.000910	0.044
30	26	0.001545	0.563	40	29	0.001901	0.49	50	32	0.000919	0.392
30	29	0.001628	0.668	40	32	0.002147	0.504	50	35	0.000938	0.480
30	32	0.001752	0.677	40	35	0.002335	0.501	50	38	0.000949	0.486
30	35	0.001932	0.691	40	38	0.002440	0.501	50	41	0.000976	0.496
30	38	0.002025	0.698	40	41	0.002456	0.501	50	44	0.001002	0.501
30	41	0.002035	0.703	40	44	0.002426	0.501	50	47	0.001025	0.503
30	44	0.002047	0.710	40	47	0.002465	0.501	50	50	0.001020	0.510
30	47	0.002072	0.713	40	50	0.002473	0.501	50	53	0.001022	0.511
30	50	0.002115	0.714	40	53	0.002500	0.501	50	56	0.001025	0.512
30	53	0.002256	0.716	40	56	0.002496	0.501	50	59	0.001028	0.513
30	56	0.002282	0.718	40	59	0.002500	0.501				
30	59	0.002300	0.719								

RR (%)	DT (day)	FSH (mstr.)	CW (mm)	RR (%)	DT (day)	FSH (mstr.)	CW (mm)	RR (%)	DT (day)	FSH (mstr.)	CW (mm)
60	32	0.001899	0.021	70	35	0.002482	0.020	80	35	0.002458	0.013
60	35	0.002014	0.291	70	38	0.002501	0.192	80	38	0.002476	0.128
60	38	0.002145	0.356	70	41	0.002504	0.204	80	41	0.002479	0.136
60	41	0.002265	0.361	70	44	0.002504	0.209	80	44	0.002479	0.139
60	44	0.002290	0.368	70	47	0.002506	0.211	80	47	0.002481	0.141
60	47	0.002437	0.371	70	50	0.002508	0.213	80	50	0.002483	0.142
60	50	0.002443	0.373	70	53	0.002510	0.214	80	53	0.002485	0.143
60	53	0.002485	0.378	70	56	0.002516	0.216	80	56	0.002491	0.144
60	56	0.002501	0.379	70	59	0.002520	0.217	80	59	0.002495	0.145
60	59	0.002519	0.380								

RR (%)	DT (day)	FSH (mstr.)	CW (mm)	RR (%)	DT (day)	FSH (mstr.)	CW (mm)
90	38	0.002724	0.005	100	41	0.002808	0.006
90	41	0.002727	0.073	100	44	0.002809	0.054
90	44	0.002727	0.090	100	47	0.002811	0.057
90	47	0.002729	0.091	100	50	0.002813	0.058
90	50	0.002731	0.093	100	53	0.002815	0.059

Table 2 continued

RR (%)	DT (day)	FSH (mstr.)	CW (mm)	RR (%)	DT (day)	FSH (mstr.)	CW (mm)
90	53	0.002733	0.093	100	56	0.002823	0.060
90	56	0.002740	0.094	100	59	0.002826	0.060
90	59	0.002744	0.095				

Table 3 The comparison of performances of the trial models

Model	Method	Membership function	Function type	Range of influence	Squash factor	Accept ratio	Reject ratio	RMSE (test)	R^2 (test)
Grid1	Grid partition	Gaussian1	Constant	–	–	–	–	0.050131	0.984891
Grid2	Grid partition	Gaussian1	Linear	–	–	–	–	0.059401	0.980169
Grid3	Grid partition	Gaussian2	Constant	–	–	–	–	0.059376	0.978733
Grid4	Grid partition	Gaussian2	Linear	–	–	–	–	0.056697	0.981113
Grid5	Grid partition	Sigmoid	Constant	–	–	–	–	0.065139	0.974344
Grid6	Grid partition	Sigmoid	Linear	–	–	–	–	0.078523	0.965809
Sub1	Sub-clustering	Gaussian1	Constant	0.5	1.25	0.5	0.15	0.075926	0.965028
Sub2	Sub-clustering	Gaussian1	Constant	0.4	1.25	0.5	0.15	0.046508	0.986872
Sub3	Sub-clustering	Gaussian1	Constant	0.3	1.25	0.5	0.15	0.039273	0.990649
Sub4	Sub-clustering	Gaussian1	Constant	0.2	1.25	0.5	0.15	0.037730	0.991889
Sub5	Sub-clustering	Gaussian1	Constant	0.2	1.25	0.5	0.15	0.038503	0.991251
Sub6	Sub-clustering	Gaussian1	Constant	0.6	1.25	0.5	0.15	0.075832	0.965202
Sub7	Sub-clustering	Gaussian1	Constant	0.7	1.25	0.5	0.15	0.096375	0.943681

replacement. The porosity of the mortars increases with the increase in GBFS aggregate content. The reason of this statement is the coarser gradation of GBFS than the one of CEN reference natural sand. The gradations of GBFS and reference sand are given in Table 4.

Root-mean-square error (RMSE), the absolute fraction of variance (R^2) and mean absolute percentage error (MAPE) are used to evaluate the performance of the model as their extensions with their comparisons are given in Table 5. Similar conclusions and explanations as above can be given for this case also. It can be pointed out that the model parameters are chosen after trying different parameters such as sub-clustering, other kinds of MFs, different numbers of MFs and iterations. The performance values are checked, and it is decided that the best solutions and predictions can be obtained by using grid partition method, with five Gaussian MFs and hybrid method. However, due to the irregular distribution of input FS, such RMSE, R^2 and MAPE values are obtained by using Eqs. 7, 8 and 9. On the other hand, it should still be indicated that the prediction results are acceptable and close to the experimental crack width results obtained from ring test.

$$RMSE = \sqrt{\frac{1}{N}\sum_{i=1}^{N}(y_{i-}\hat{y}_i)^2} \tag{7}$$

$$R^2 = \frac{\left(n\sum t_i o_i - \sum t_i \sum o_i\right)^2}{\left(n\sum t_i^2 - (\sum t_i)^2\right)\left(n\sum o_i^2 - (\sum o_i)^2\right)} \tag{8}$$

$$MAPE = \frac{1}{n}\left[\frac{\sum_{i=1}^{n}|t_i - o_i|}{\sum_{i=1}^{n}t_i} \times 100\right] \tag{9}$$

Finally, it can be said that the predicted and experimental results are close to each other for most of the testing data and ANFIS can be employed to predict the drying shrinkage crack widths without attempting ring test (heavy molds and long time as at least 60 days) by determining only the free shrinkage length changes. Furthermore, the prediction results give an opinion about the cracking performance of such mortars and ANFIS could be adapted for predicting the crack widths of different types of concretes and mortars. Besides, the model depends on RR of GBFS, DT of specimen and FS of mortar rather than mixture properties such as aggregate, water and cement contents, w/c ratio and admixture type. which may differ from mortar to mortar or concrete to concrete. This means that the model proposed can be generalized for all kinds of mortars. However, new crack width prediction models should be developed for concrete considering properties wisely that may be used as input data. On the other hand, it is possible to construct generalized ANFIS models to predict shrinkage cracking of

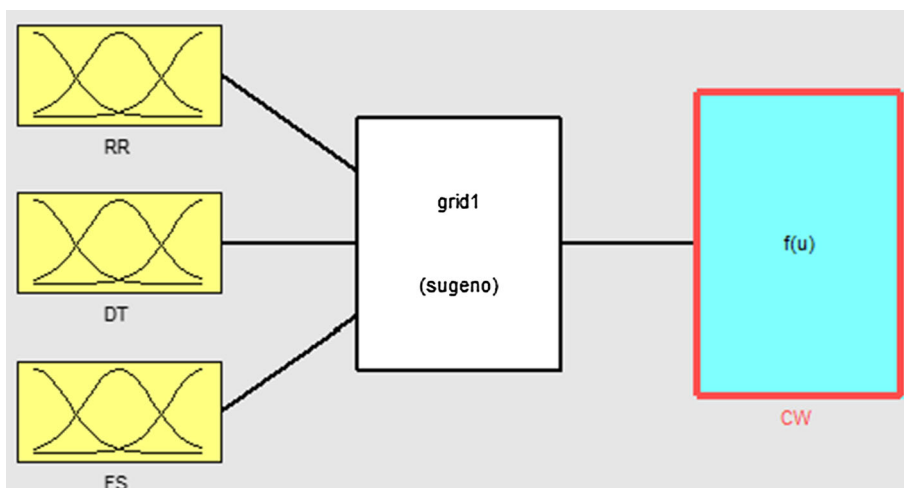**Fig. 4** Schematic demonstration of the model

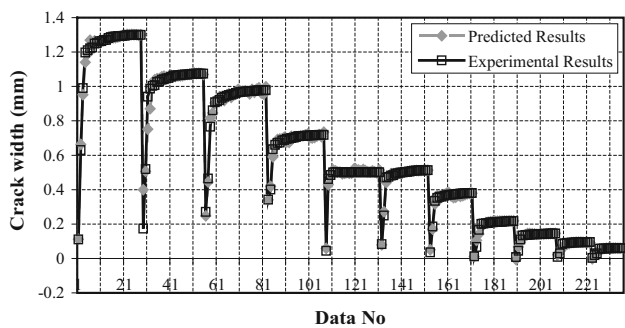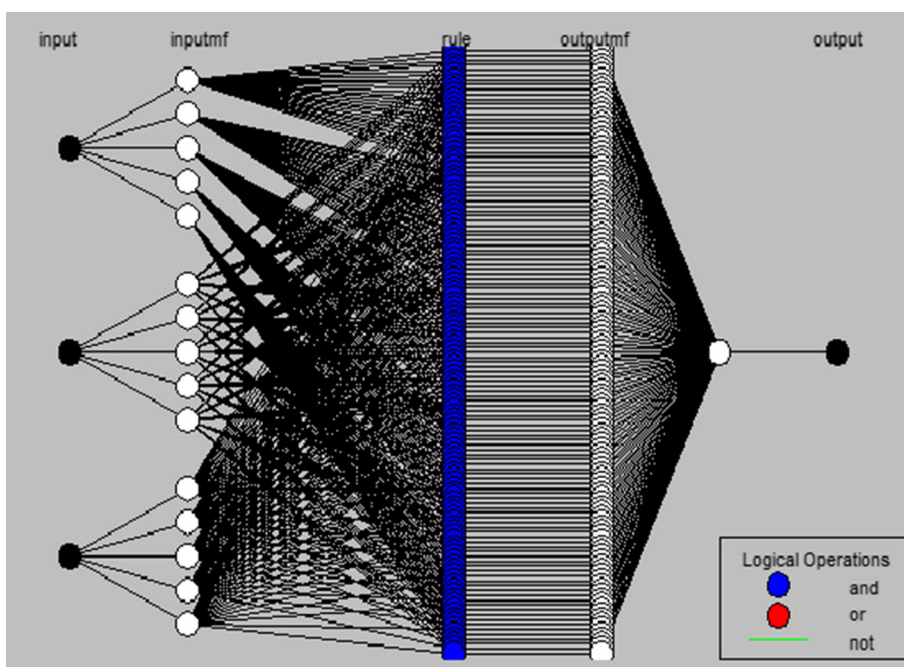**Fig. 5** Structure of the ANFIS model

Fig. 6 Comparison of the predicted and experimental results after training

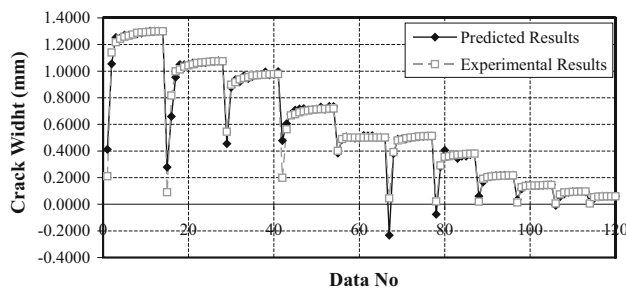**Fig. 7** Comparison of the predicted and experimental results after testing

Table 4 The gradations of sand and GBFS

Sieve analysis			
GBFS		**Reference natural sand**	
Sieve interval (mm)	Cumulative retaining above sieve (%)	Sieve interval (mm)	Cumulative retaining above sieve (%)
4	21.2	2	0
2	79.4	1.6	7 ± 5
1	98.4	1	33 ± 5
0.5	99.9	0.5	67 ± 5
0.25	100	0.16	87 ± 5
0.125	100	0.08	99 ± 1
Pan	100	Pan	–

Table 5 RMSE, R^2 and MAPE values of the ANFIS model

Performance value	Training	Testing
RMSE	0.0241981	0.0501315
R^2	0.9964013	0.9848913
MAPE	0.0000034	22.0284662

mortars and concretes due to the nature of ANFIS. Additionally, the model proposed can be used to estimate the shrinkage cracking of GBFS fine aggregate mortars which may possibly be used for producing plasters and make it available to take precautions before producing these types of plasters. This situation would gain economical and time-savings. Consequently, it would be available and possible to prevent required precautions in order to improve the shrinkage cracking performance and thus, the durability of mortar or concrete.

5 Conclusions

It is extremely difficult to take into account of all either controllable or uncontrollable parameters for the prediction of drying shrinkage cracking. Some empirical models have been widely used for drying shrinkage prediction and rarely used for drying shrinkage cracking. In this study, the drying shrinkage crack widths obtained from the ring test could easily and accurately be predicted.

Consequently, the ANFIS ring test restrained drying shrinkage crack width prediction model developed for GBFS mortars can be a useful tool for engineers as a preliminary guide for evaluating the effects of drying shrinkage cracking on mortars considering the GBFS replacement, drying time and the possible length changes. Moreover, improvements and modifications for the model may be achieved by constructing a wider database and

including additional input variables such as environmental conditions and mixture compositions even if they were expressed linguistically. Besides, this developed model or the improved one can be adapted for different kinds of mortars and concretes exposed to different environment conditions and incorporating different types of materials such as cements, aggregates, mineral and chemical admixtures, bottom ash, fly ash, rubber and crushed tile, as mineral admixture or aggregate, having different water to cement ratios, different sizes of aggregates, water content, cement content. Briefly, it is possible to construct different types of models predicting different properties of mortars or concretes having different properties under different circumstances. In this study, this advantage has been used for predicting the drying shrinkage crack widths of GBFS mortars.

Besides, these types of drying shrinkage crack width prediction models would help the mortar–concrete designers and the producers to consider precautions before production without losing time and money. In addition, they would contribute to the durability of the material by preventing or reducing the shrinkage cracking before producing the mortar and concrete. Therefore, they can also contribute to the sustainable development by making it possible to gain economical, environmental and technical advantages in production.

References

1. Topçu İB (2006) Materials of construction and concrete. Uğur Offset, Eskişehir
2. Topçu İB (2006) Concrete technology. Uğur Offset, Eskişehir
3. Atiş CD, Kiliç A, Sevim UK (2004) Strength and shrinkage properties of mortar containing a nonstandard high-calcium fly ash. Cem Concr Res 34(1):99–102
4. Kayali O, Haque MN, Zhu B (1999) Drying shrinkage of fibre reinforced lightweight aggregate concrete containing fly ash. Cem Concr Res 29(11):1835–1840
5. McCarthy MJ, Dhir RK (2005) Development of high volume fly ash cements for use in concrete construction. Fuel 84(11):1423–1432
6. Termkhajornkit P, Nawa T, Nakai M, Saito T (2005) Effect of fly ash on autogenous shrinkage. Cem Concr Res 35(3):473–482
7. Filho RDTP, Ghavami K, Sanjuan MA, England GL (2005) Free, restrained and drying shrinkage of cement mortar composites reinforced with vegetable fibres. Cem Concr Compos 27(5):537–546
8. Gesoğlu M, Özturan T, Güneyisi E (2006) Effects of cold-bonded fly ash aggregate properties on the shrinkage cracking of light-weight concretes. Cem Concr Compos 28(7):598–605
9. Bissonnette B, Pierre P, Pigeon M (1999) Influence of key parameters on drying shrinkage of cementitious materials. Cem Concr Res 29(10):1655–1662
10. Jiang Z, Sun Z, Wang P (2005) Autogenous relative humidity change and autogenous shrinkage of high-performance cement pastes. Cem Concr Res 35(8):1539–1545

11. Turatsinze A, Bonnet S, Granju J-L (2007) Potential of rubber aggregates to modify properties of cement based-mortars: improvement in cracking shrinkage resistance. Constr Build Mater 21(1):176–181

12. Kanna V, Olson RA, Jennings HM (1998) Effect of shrinkage and moisture content on the physical characteristics of blended cement mortars. Cem Concr Res 28(10):1467–1477

13. Bisschop J, van Mier JGM (2002) How to study drying shrinkage microcracking in cement-based materials using optical and scanning electron microscopy. Cem Concr Res 32(2):279–287

14. Hossain AB, Weiss J (2006) The role of specimen geometry and boundary conditions on stress development and cracking in the restrained ring test. Cem Concr Res 36(1):189–199

15. Yüksel İ, Özkan Ö, Bilir T (2006) Use of granulated blast furnace slag in concrete as fine aggregate. ACI Mater J 103(3):203–208

16. Yüksel İ, Bilir T (2007) Usage of industrial by-products to produce plain concrete elements. Constr Build Mater 21(3):686–694

17. Yüksel İ, Bilir T, Özkan Ö (2007) Durability of concrete incorporating non-ground blast furnace slag and bottom ash as fine aggregate. Build Environ 42(7):2651–2659

18. Topçu İB, Boğa AR, Bilir T (2008) Alkali–silica reactions of mortars produced by using waste glass as fine aggregate and admixtures such as fly ash and Li_2CO_3. Waste Manag 28(5):878–884

19. Topçu İB, Bilir T (2007) Effect of slag fineness on durability of mortars. J Zhejiang Univ Sci A 8(11):1725–1730

20. Topçu İB, Canbaz M (2003) Properties of concrete containing waste glass. Cem Concr Res 34(2):267–274

21. Yüksel İ, Genç A (2007) Properties of concrete containing non-ground ash and slag as fine aggregate. ACI Mater J 104(4):397–403

22. Collins F, Sanjayan JG (2000) Cracking tendency of alkali-activated slag concrete subjected to restrained shrinkage. Cem Concr Res 30(5):791–798

23. See HT, Attiogbe EK, Miltenberger MA (2003) Shrinkage cracking characteristics of concrete using ring specimens. ACI Mater J 100(3):239–245

24. Shah SP, Karaguler ME, Sarigaphuti M (1992) Effects of shrinkage-reducing admixtures on restrained shrinkage cracking of concrete. ACI Mater J 89(3):289–295

25. Appa Rao G (2001) Long-term drying shrinkage of mortar-influence of silica fume and size of fine aggregate. Cem Concr Res 31(2):171–175

26. Almudaiheem JA, Hansen W (1987) Effect of specimen size and shape on drying shrinkage of concrete. ACI Mater J 84(2):130–135

27. Mesbah HA, Buyle-Bodin F (1999) Efficiency of polypropylene and metallic fibres on control of shrinkage and cracking of recycled aggregate mortars. Constr Build Mater 31(8):439–447

28. Najm H, Balaguru P (2002) Effect of large-diameter polymeric fibers on shrinkage cracking of cement composites. ACI Mater J 99(4):345–351

29. Voigt T, Bui VK, Shah SP (2004) Drying shrinkage of concrete reinforced with fibers and welded-wire fabric. ACI Mater J 101(3):233–241

30. Swamy RN, Stavrides H (1979) Influence of fiber reinforcement on restrained shrinkage and cracking. ACI Mater J 76(3):443–460

31. Bloom R, Bentur A (1995) Free and restrained shrinkage of normal and high-strength concrete. ACI Mater J 92(2):211–217

32. El Hindy E, Miao B, Chaallal O, Aitcin P-C (1994) Drying shrinkage of ready-mixed high-performance concrete. ACI Mater J 91(3):300–305

33. Lopez M, Kahn LF, Kurtis KE (2004) Creep and shrinkage of high-performance lightweight concrete. ACI Mater J 101(5):391–399

34. Zhang M-H, Li L, Paramasivam P (2005) Shrinkage of high-strength lightweight aggregate concrete exposed to dry environment. ACI Mater J 102(2):86–92

35. Fernandez-Gomez J, Landsberger GA (2007) Evaluation of shrinkage prediction models for self-consolidating concrete. ACI Mater J 104(5):464–473

36. Torrenti JM, Granger L, Diruy M, Genin P (1999) Modeling concrete shrinkage under variable ambient conditions. ACI Mater J 96(1):35–39

37. Collins F, Sanjayan JG (2000) Numerical modeling of alkali-activated slag concrete beams subjected to restrained shrinkage. ACI Mater J 97(5):594–602

38. Ojdrovic RP, Zarghamee MS (1996) Concrete creep and shrinkage prediction from short-term tests. ACI Mater J 93(2):169–177

39. Carlson RW, Reading TJ (1988) Model study of shrinkage cracking in concrete building walls. ACI Mater J 85(4):395–404

40. McDonald DB, Roper H (1993) Accuracy of prediction models for shrinkage of concrete. ACI Mater J 90(3):265–271

41. Barr B, Hoseinian SB, Beygi MA (2003) Shrinkage of concrete stored in natural environments. Cem Concr Compos 25(1):19–29

42. Gardner NJ, Lockman MJ (2001) Design provisions for drying shrinkage and creep of normal-strength concrete. ACI Mater J 98(2):159–167

43. Huo XS, Al-Omaishi N, Tadros MK (2001) Creep, shrinkage, and modulus of elasticity of high-performance concrete. ACI Mater J 98(6):440–449

44. Rouse JM, Billington SL (2007) Creep and shrinkage of high-performance fiber-reinforced cementitious composites. ACI Mater J 104(2):129–134

45. Al Rawi RS, Kheder GF (1990) Control of cracking due to volume change in base-restrained concrete members. ACI Mater J 87(4):397–405

46. Nejadi S, Gilbert I (2004) Shrinkage cracking and crack control in restrained reinforced concrete members. ACI Mater J 101(6):840–845

47. Shah SP, Ouyang C, Marikunte S, Yang W, Becq-Giraudon E (1998) A method to predict shrinkage cracking of concrete. ACI Mater J 95(4):339–346

48. Jang RJS, Sun CT, Mizutani E (1997) Neuro-fuzzy and soft computing. Prentice-Hall, Upper Saddle River

49. İphar M, Yavuz M, Ak H (2008) Prediction of ground vibrations resulting from the blasting operations in an open-pit mine by adaptive neuro-fuzzy inference system. Eng Geol 56(1):97–107

50. Jang RJS (1993) ANFIS: adaptive-network-based fuzzy inference system. IEEE Trans Syst Man Cybern 23(3):665–685

51. Topçu İB, Sarıdemir M (2008) Prediction of rubberized concrete properties using artificial neural network and fuzzy logic. Constr Build Mater 22(4):532–540

52. Topçu İB, Sarıdemir M (2007) Prediction of waste AAC aggregate concrete properties using artificial neural network and fuzzy logic. Comput Mater Sci 41(1):117–125

53. Turkish Standards Institute (2002) Turkish standard for methods of testing cement-part 1: determination of strength. Standard no TS EN 196-1

54. ASTM (2006) Standard test method for length change of hardened hydraulic-cement mortar and concrete. Standard no ASTM C157/C157 M-06